ISSN 1846-6168 (Print), ISSN 1848-5588 (Online)
https://doi.org/10.31803/tg-20230508230247

Preliminary communication
Received: 2023-05-08, Accepted: 2023-05-12

Optimisation of Parameters for Metal Part Cutting on a CNC Plasma Cutting Machine

Hrvoje Cajner*, Vid Križanić, Tihomir Opetuk, Maja Trstenjak

Abstract: This paper refers to the topic of determining the kerf value and axis accuracy of a CNC plasma cutter for the cutting of 2, 4 and 6 mm thick plates of construction steel, aluminum and stainless steel. After the thorough description of the researched materials, a detailed experiment plan was created in the Design-Expert software package. After cutting the test samples the data were measured. Upon completion of the cutting, all test samples were measured, and the data regarding their dimensional deviations on x and y-axis and bore diameter deviations was tabularly shown and analysed with the Design – Expert software. Statistical analysis of the measured data was made so that the optimal kerf values and the equations which describe dimensional deviations for each material and thickness could be made, based on the dimensional deviation of the test samples. Along with the kerf values, analysis has also given insight in the accuracy of the x and y-axis of the machine. Finally, an algorithm for optimizing multiple criteria was utilized to determine the ideal kerf value for each material and thickness. The objective was to identify the precise kerf value that results in the highest possible accuracy for the dimensions of the workpiece in both the x and y directions, as well as for the bore diameter.

Keywords: dimensional accuracy; CNC plasma cutter; kerf; process optimisation

1 INTRODUCTION

The feasibility and quality of plasma cutting are determined by numerous parameters, with the most important ones being [1,2]: plasma arc power, cutting speed, choice of plasma gas, choice of secondary gas (if used), nozzle-to-workpiece distance, kerf width and angle of cut. Plasma arc power is derived from the power supply typically ranging between 200 VDC and 400 VDC (depending on operator settings), although these values can be lower than 200 VDC or higher than 400 VDC. The operator determines the amount of electric current required for cutting, so for thinner materials, they may require less electric current from the power source, whereas for cutting thicker materials, they may require more electric current [3]. Power sources vary greatly in terms of the power and current strength they can use to create a plasma arc. For example, there are smaller power supplies with 6.5 kW power, intended for cutting softer steels and thinner aluminum (up to about 15 mm) with a current of 10 to 45 A, but there are also larger power supplies with power greater than 66.5 kW that can cut stainless steel with a thickness of 75 mm with a current of up to 300 A [4].

The primary objective of any processing method is to attain optimal quality of the final product, while maintaining maximum productivity. In the context of plasma cutting, it is crucial to consider multiple factors, such as achieving the highest possible lifespan of consumables (i.e., electrodes and nozzles), minimizing the quantity of slag on the workpiece, reducing post-processing of the cut specimen, minimizing the achievable kerf width, and ensuring dimensional and geometric precision of the cut specimen [5]. The cutting speed directly impacts these factors, as the adjustment of the cutting speed alters the kerf width, amount of slag, lifespan of consumables, and other related parameters. Power supply manufacturers typically provide recommended current, voltage, and cutting speed values for each specific model of power supply, based on the material being cut and its thickness. However, operators may adjust these values based on their own experiences, considering electrode and nozzle wear, ambient humidity and temperature during cutting, surface conditions of the material being cut (e.g., presence of impurities and/or corrosion), among others.

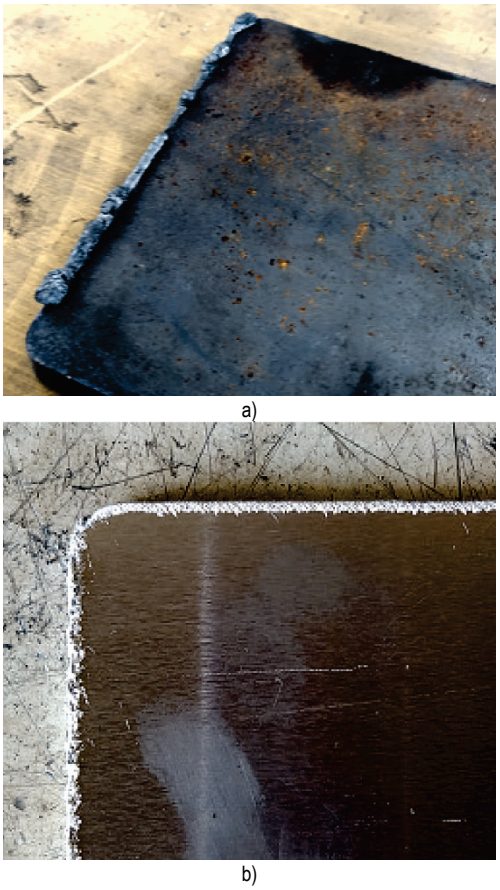

a)

b)

Figure 1 Common issues during machining process using suboptimal settings: a) The accumulation of slag on the underside of the cut specimen due to insufficient cutting speed, b) Slag on the upper side of the workpiece due to excessive cutting speed.

When conducting plasma cutting, it is recommended to process at the maximum possible speed, while ensuring that the final quality of the cut specimen is not compromised.

Reduction in cutting speed results in increased slag on the underside of the workpiece (Fig. 1a), leading to greater need for post-processing of the cut specimen, and potentially causing plasma arc deflection, which accelerates the erosion of electrodes and nozzles [6]. Additionally, excessive cutting speed may prevent successful cutting, as the material is incompletely melted and removed from the cutting zone, as seen in Fig. 1b.

The kerf refers to the geometry of the cut on a material and has its characteristic dimensions - width and angle. The width and angle of the kerf are correlated with other parameters, and their values are influenced by the cutting power (used current), cutting speed, type and thickness of the material, distance between the nozzle and the workpiece, and the gas used. The angle of the kerf is most easily observed in plasma cutting with air. As shown in Fig. 2, the width of the kerf at the top of the workpiece is greater than at the bottom, indicating that the cut is made at an angle [7].

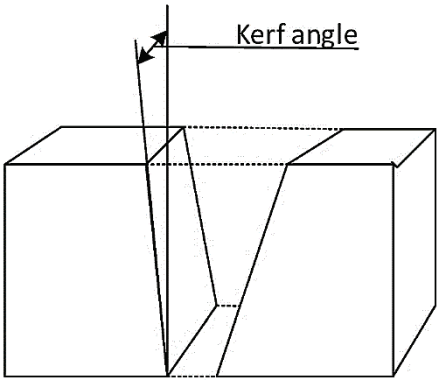

Figure 2 Angle of the kerf in case of plasma cutting with air [7]

Additional factors that can cause unfavourable kerf widths and angles include worn-out machine parts, possible protrusions or indentations on the workpiece that the height control system does not register quickly enough, the use of the wrong gas distributor, or non-compliance of the torch with respect to the workpiece. Essentially, low height and/or too slow cutting speed cause a negative kerf angle, while too high height and/or cutting speed cause a positive angle. Therefore, if a negative kerf angle occurs on the cut specimen, a potential solution to correct the cut quality is to increase the height or cutting speed, while decreasing the height or speed can be used when a positive kerf angle is present.

When it comes to the kerf width and angle, it is essential to find a compromise between quantity and quality, meaning it is necessary to find a cutting speed value that satisfies productivity criteria, but still achieves satisfactory cut quality and an acceptable kerf angle. It should be noted that at significantly higher cutting speeds than recommended, regardless of the demands on the quality of the cut specimen, the kerf angle might increase to the extent that the cut edges on the bottom of the workpiece come too close together and thereby got fused [7]. The literature provides many diagrams in which the amount of the kerf angle is calculated depending on the cutting speed specific workpiece material and thickness [1, 8-10]. The objective of this experiment, notwithstanding all the previously mentioned factors, was to identify the optimal or nearly optimal process setup to attain satisfactory dimensional precision of the workpiece focusing on parameter that deals with kerf.

2 DESIGN OF EXPERIMENT

The primary goal of the experiment is to determine the optimal values of the kerf parameter for different materials and thicknesses, based on the measurements of rectangular test samples cut by plasma arc, assuming that the cutting speed, current strength, and voltage are constant for each material and its thickness. The secondary goal of this experiment is to determine the accuracy of the x and y axes of the machine. The measurements are used to test whether the cut along the *x*-axis has greater accuracy than the cut along the *y*-axis, which can help operators in the company orient the cut specimens, so that the sides of the workpieces that have stricter accuracy requirements are positioned along the more accurate axis of the machine. Improved machine accuracy results in reduced time spent on welding and assembly, as well as decreased consumption of additional materials during welding.

The experiment was conducted on CNC plasma cutting machine is primarily used for cutting structural steel, aluminum and stainless steel up to a thickness of 10 mm, although it has the capability to cut thicker materials. The machine's construction consists of a table made by the Chinese manufacturer HectMac in a welded design that can accommodate sheet materials with maximum dimensions of 1500 × 4000 mm, and a console that provides movement along the x-axis, i.e. along the length of the table provided by HIWIN manufacturer. On the console, there is also a pair of guides, each with a slider, for movement along the x and y axis. The torch as well as the power supply are produced by Hypertherm. Before starting the process of cutting, the CNC operator must adjust the required amount of electric current and plasma gas flow (in this case air) on the power supply and define the cutting speed, value of kerf, voltage value, time delay, and initial nozzle height when piercing the material on the machine control unit. Some CNC control units work in combination with software packages that have libraries storing kerf values for each processed material and its thickness, but the specific machine control unit does not have this option, so it is necessary to manually enter the value of kerf before running the program. The wrong value of the kerf can lead to poor workpiece quality.

To determine value of kerf, experiment with test samples which are cut from various materials of different thicknesses was conducted. The test specimens are rectangular plates with dimensions of 80 × 60 mm and a central bore with a diameter of 12 mm, shown in Fig. 3. The specimens are of the same dimensions for each material and thickness used in the experiment, but their orientation differs, thereby determining the accuracy of the *x* and *y* axes of the machine, which is also the secondary goal of the experiment.

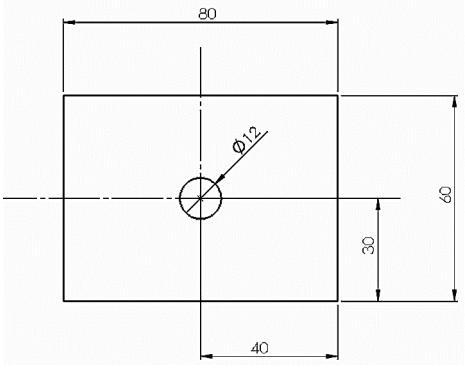

Figure 3 The test specimen

The three-level full factorial design with replications were chosen to analyse the effects and conduct optimisation (Tab. 1). The parameter of the kerf was varied over 3 level which are 0.25, 0.425 and 0.6 mm. The materials that are being used for the purposes of this experiment are structural steel marked S235JR, aluminum marked AlMg3, and stainless steel marked X5CrNiMo17-12-2. Testing is carried out for each material in three thicknesses: 2, 4, and 6 mm, and nine test samples are cut from each thickness, for 81 experiments. The response variables are obtained as deviation from the nominal dimension along the *x* and *y*-axis, as well as deviation from the nominal diameter of the bore.

Table 1 Experimental setup

Factor	Name	Units	Minimum	Centre	Maximum
A:	KERF	mm	0,25	0,425	0,6
B:	Thickness	mm	2	4	6
C:	Material	-	Con. steel	Stainless steel	Aluminum
Response	Label	Units			
Y1	Δx	mm			
Y2	Δy	mm			
Y3	$\Delta \Phi$	mm			

3 ANALYSIS OF THE RESULTS

After cutting all the test specimens, a final grinding process is carried out on the upper and lower sides using an angle grinder, in order to remove slag from the plates without altering their geometry and dimensions of length and width. The cut and ground test specimens are then measured with a vernier caliper to a precision of 0.02 mm for their outer dimensions (length and width, i.e. outer dimensions along the *x* and *y*-axes) and bore width along the x and y axes.

The results of the experiment are presented in Tab. 2.

Table 2 Results of the experiment

	Orientation	A: Kerf (mm)	B: Thickness (mm)	C: Material	Δx (mm)	Δy (mm)	$\Delta \Phi$ (mm)
1	X-y	0.25	2	Aluminum	-0.16	-0.38	1.24
2	X-y	0.425	6	Con. steel	0.64	0.52	0.09
3	X-y	0.6	6	Aluminum	0.48	0.04	-0.57
4	X-y	0.425	4	Aluminum	0.12	0	0.66
5	X-y	0.6	4	Con. steel	0.56	0.28	-0.24
6	X-y	0.25	2	Stainless steel	0.12	-0.44	0.83
7	X-y	0.25	4	Con. steel	-0.32	-0.38	0.4
8	X-y	0.6	2	Aluminum	0.64	0.34	0.56
9	X-y	0.425	2	Con. steel	0.42	0.34	0.63
10	X-y	0.25	6	Aluminum	-0.68	0.68	0.2
11	X-y	0.6	2	Stainless steel	1.14	0.4	0.1
12	X-y	0.6	6	Stainless steel	-0.34	-0.76	-0.69
13	X-y	0.425	4	Steel	-0.1	-0.06	0.01
14	X-y	0.25	6	Stainless steel	-0.12	-0.82	0
15	y-X	0.425	4	Stainless steel	-0.28	-0.04	0.09
16	y-X	0.425	2	Stainless steel	0.44	0.82	0.71
17	y-X	0.6	6	Steel	0.56	0	-0.6
18	y-X	0.425	2	Aluminum	0.44	-0.28	0.82
19	y-X	0.6	4	Aluminum	0.34	0.74	0.08
20	y-X	0.6	2	Con. steel	0.6	0.68	0.27
21	y-X	0.25	6	Con. steel	-0.56	-0.38	0.01
22	y-X	0.425	6	Stainless steel	-0.8	-0.28	-0.41
23	y-X	0.25	4	Stainless steel	-0.08	-0.5	0.46
24	y-X	0.6	4	Stainless steel	-0.14	0.36	-0.18
25	y-X	0.25	4	Aluminum	0	0.76	0.93
26	y-X	0.425	6	Aluminum	-0.28	0.2	-0.11
27	y-X	0.25	2	Con. steel	0.18	-0.34	0.93
28	y-X	0.25	2	Con. steel	-0.1	0.02	0.9
29	y-X	0.6	2	Con. steel	0.78	0.66	0.23
30	y-X	0.25	6	Con. steel	-0.24	-0.68	0.06
31	y-X	0.6	6	Con. steel	0.12	0.06	-0.62
32	X-y	0.425	2	Con. steel	0.46	0	0.65
33	X-y	0.25	4	Con. steel	-0.54	-0.68	0.39
34	X-y	0.6	4	Con. steel	0.56	-0.04	-0.2
35	X-y	0.425	6	Con. steel	0.08	0.1	-0.11
36	X-y	0.425	4	Con. steel	0	-0.08	0.15
37	X-y	0.25	2	Stainless steel	0.18	-0.12	0.97
38	X-y	0.6	2	Stainless steel	0.94	0.64	0.12
39	X-y	0.25	6	Stainless steel	-0.98	-0.86	-0.1
40	X-y	0.6	6	Stainless steel	0.02	-0.32	-0.72
41	y-X	0.425	2	Stainless steel	0.18	-0.18	0.38
42	y-X	0.25	4	Stainless steel	-0.7	-0.3	0.52
43	y-X	0.6	4	Stainless steel	0.26	0.08	-0.26
44	y-X	0.425	6	Stainless steel	-0.28	0.34	-0.68
45	y-X	0.425	4	Stainless steel	-0.64	-0.18	0.05
46	X-y	0.25	2	Aluminum	0.02	-0.22	1.09
47	X-y	0.6	2	Aluminum	0.68	0.18	0.61
48	X-y	0.25	6	Aluminum	-0.28	0.26	0.34
49	X-y	0.6	6	Aluminum	0.3	1.52	-0.3
50	y-X	0.425	2	Aluminum	0.6	0.06	0.81
51	y-X	0.25	4	Aluminum	-0.56	-0.52	0.8
52	y-X	0.6	4	Aluminum	0.4	1	0.14
53	y-X	0.425	6	Aluminum	-0.04	-0.44	0.11
54	X-y	0.425	4	Aluminum	-0.26	-0.22	0.15
55	y-X	0.25	2	Con. steel	0	-0.14	1.01
56	y-X	0.6	2	Con. steel	0.34	0.48	0.2
57	y-X	0.25	6	Con. steel	-0.1	-0.68	0.11
58	y-X	0.6	6	Con. steel	0.36	0.04	-0.58
59	X-y	0.425	2	Con. steel	0.38	0.1	0.65
60	X-y	0.25	4	Con. steel	-0.44	-0.32	0.55
61	X-y	0.6	4	Con. steel	0.24	0.48	-0.18
62	X-y	0.425	6	Con. steel	-0.04	0.54	-0.18
63	X-y	0.425	4	Con. steel	0.08	0.2	0.04
64	X-y	0.25	2	Stainless steel	-0.08	0.16	0.98
65	X-y	0.6	2	Stainless steel	0.66	0.96	0.23
66	X-y	0.25	6	Stainless steel	-0.44	-0.96	-0.25
67	X-y	0.6	6	Stainless steel	0	0.22	-0.94
68	y-X	0.425	2	Stainless steel	0.14	-0.02	0.65
69	y-X	0.25	4	Stainless steel	-0.38	-0.32	0.44
70	y-X	0.6	4	Stainless steel	0.06	0.08	-0.02
71	y-X	0.425	6	Stainless steel			

	Orientation	A: Kerf (mm)	B: Thickness (mm)	C: Material	Δx (mm)	Δy (mm)	$\Delta \Phi$ (mm)
72	y-X	0.425	4	Stainless steel	-0.34	-0.04	0.19
73	X-y	0.25	2	Aluminum	-0.14	-0.26	1.23
74	X-y	0.6	2	Aluminum	0.52	0.38	0.55
75	X-y	0.25	6	Aluminum	-0.34	-0.3	0.32
76	X-y	0.6	6	Aluminum	0.32	0.12	-0.54
77	y-X	0.425	2	Aluminum	0.32	0.06	0.95
78	y-X	0.25	4	Aluminum	-0.34	-0.28	0.71
79	y-X	0.6	4	Aluminum	0.18	0.66	0.18
80	y-X	0.425	6	Aluminum			
81	X-y	0.425	4	Aluminum	0.02	0.04	0.74

Statistical analysis was performed using the Design-Expert software package, by which three-dimensional response surfaces based on regression analysis of the measured values was generated. The aforementioned response surfaces provide a visual representation of the relationship between the input factors and the dependent variables.

Data analysis was performed for each of the cut materials, across the three dependent variables deviation along the x-axis of the machine, deviation along the y-axis of the machine, and average deviation of the bore diameter.

3.1 Analysis of the Deviation along *x*-Axis

In the first case, deviations along the *x*-axis of the machine (Δx) were observed, and the results of the analysis are presented for structural steel, aluminum, and for stainless steel in the Fig. 4.

As shown in Fig. 4, the range of values for the dependent variable Δx in structural steel varied from approximately -0.45 mm to 0.6 mm, with the minimum value occurring for theoretical thicknesses between 4 and 5 mm and a kerf value of 0.25 mm, and the maximum value occurring for a thickness of 2 mm and a kerf value of 0.6 mm. Structural steels with a thickness of 6 and 4 mm exhibited both negative and positive values of Δx, depending on the kerf value input, while the values of Δx for structural steel with a thickness of 2 mm were predominantly positive. Notably, greater oscillations were observed in the experimental conditions for a thickness of 6 mm and a kerf value of 0.425 mm.

The response surface for aluminum shows some similarities to the plot for structural steel. The minimum value of Δx is approximately –0.45 mm, occurring at a material thickness of around 5 mm and a kerf value of 0.25 mm, while the maximum value of Δx is about 0.6 mm, occurring for a material thickness of 2 mm and a kerf value of 0.6 mm. One notable distinction from the plot for structural steel is that the largest oscillations in measurements were observed for aluminum with a thickness of 4 mm and a kerf value of 0.25 mm.

The observed results for stainless steel are notably different. The minimum value of Δx is –0.75 mm, occurring at a material thickness of 6 mm and a kerf value of 0.25 mm, while the maximum value of Δx is approximately 0.65 mm, occurring for a material thickness of 2 mm and a kerf value of 0.6 mm. The response surface for stainless steel exhibits a steeper slope compared to the previous response surfaces, as well as larger oscillations between the maximum and minimum values of the dependent variable Δx.

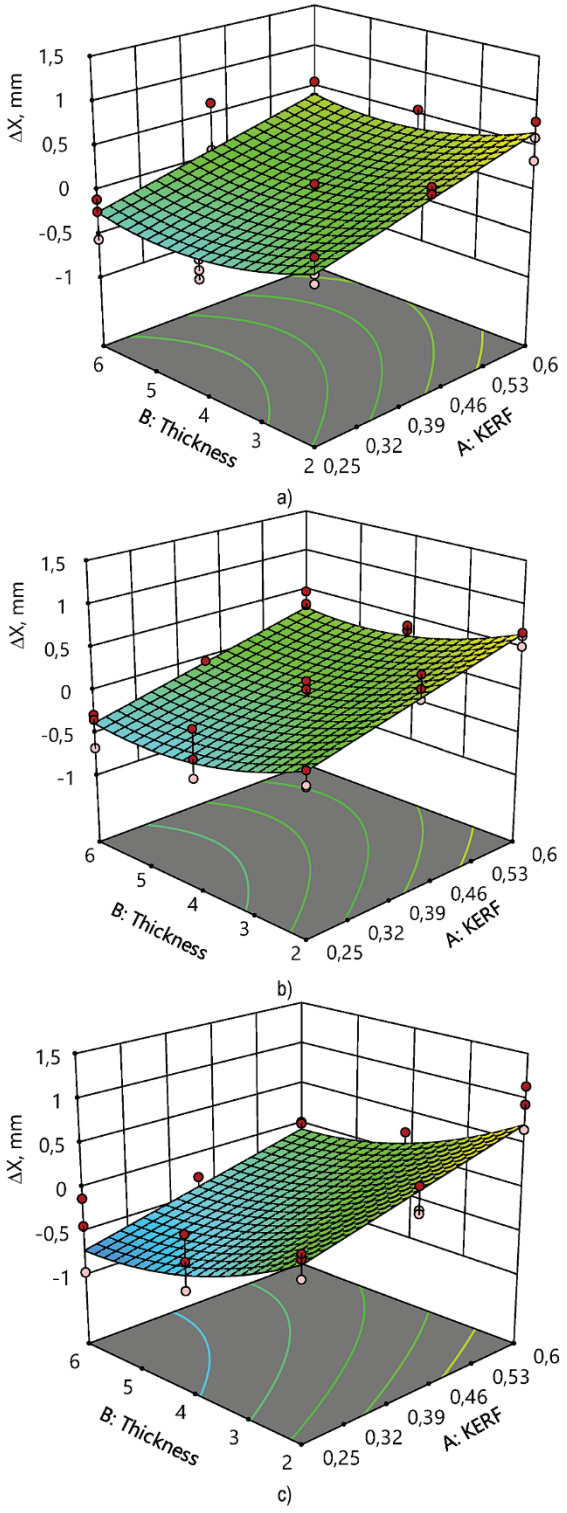

Figure 4 Response surface for deviation along x-axis for: a) Structural steel, b) Aluminum, c) Stainless steel

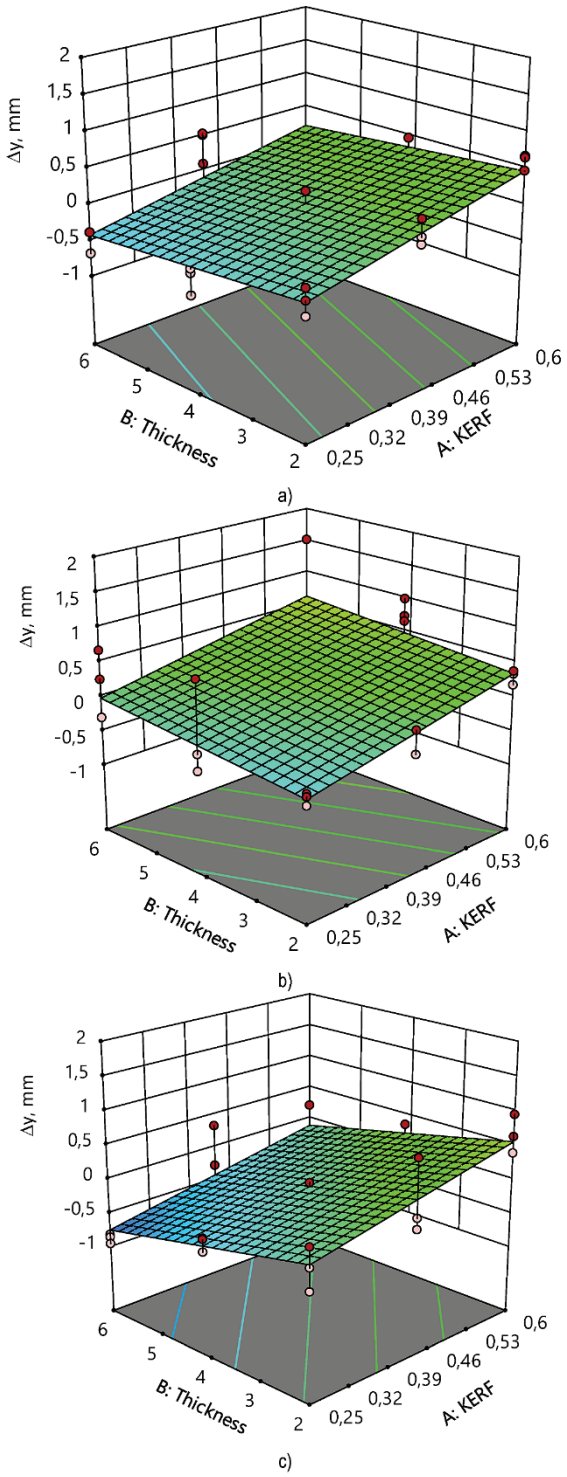

Figure 5 Response surface for deviation along y-axis for: a) Structural steel, b) Aluminum, c) Stainless steel

3.2 Analysis of the Deviation along y-Axis

In the second case, deviations along the *y*-axis of the machine (Δy) were observed, and variation between individual experimental conditions were also studied. The analysis results are presented for the structural steel, aluminum, and for stainless steel in Fig. 5. The variation between the upper and lower values of Δy for structural steel, and aluminum as well, are significantly smaller compared to those observed along the x-axis. Additionally, the inclination of the three-dimensional surface is lower, and a certain linearity is noticeable between the data obtained through regression analysis.

The variation between measured deviations for the y-axis are significantly higher for stainless steel compared to aluminum or structural steel, as is the case for the *x*-axis of the machine. Despite the larger deviations compared to other materials, the y-axis of the machine once again shows smaller overall deviations compared to the *x*-axis, even for stainless steel. That is certainly interesting fact which points out that the machine precision is slightly better along y-axis.

3.3 Analysis of the deviation of bore diameter

After analysing the deviations of individual machine axes, the deviations of bore diameter ($\Delta\Phi$) are examined. When making the bore on the test specimen, both axes must participate simultaneously so that the plasma arc can make a circular movement. Therefore, the inaccuracy of both machine axes affects the final deviation of the diameter. The nominal value of the bore diameter is 12 mm, measured along the *x* and *y* axes, and the average deviation was calculated based on the individual diameter deviations on each axis. The mentioned deviations for structural steel, aluminum, and stainless steel is presented in Fig. 6.

In case of structural steel, the response surface graph shows opposite characteristics of deviations in comparison to the deviations along the *x* or *y* axis. The values of the kerf for structural steel with thicknesses of 2 and 6 mm, which provide relatively good accuracy of the external dimensions of the test sample, have largest effect on deviations in the diameter dimension. The response surface for aluminum has similar shape but with even more emphasized extreme deviations for a material thickness of 2 mm. Like previous diagrams in case of stainless steel it has the highest extreme negative deviation. What is specific about the diameter deviation in case of stainless steel is that variations between some specific values are significantly smaller than deviations in *x* and *y* axis.

3.4 Optimisation

Based on analysed data, the multicriteria optimisation algorithm was applied in order to find the optimal value of the kerf value for each material and thickness. The goal is to find specific kerf value that gives the maximum overall accuracy of the workpiece dimensions in the *x* and *y* axes and the bore diameter as well. More precisely, the goal is to find the kerf values with minimal value of the absolute deviations of Δx, Δy and $\Delta\Phi$ for all observed workpiece materials and their thicknesses. The target value of Δx and Δy was set to 0 while the target value of $\Delta\Phi$ is set to minimal. The $\Delta\Phi$ is set to minimal due to fact that if diameter is smaller than nominal, it is possible to perform rework thus if the diameter is larger than nominal it could be costly and even impossible to do correction.

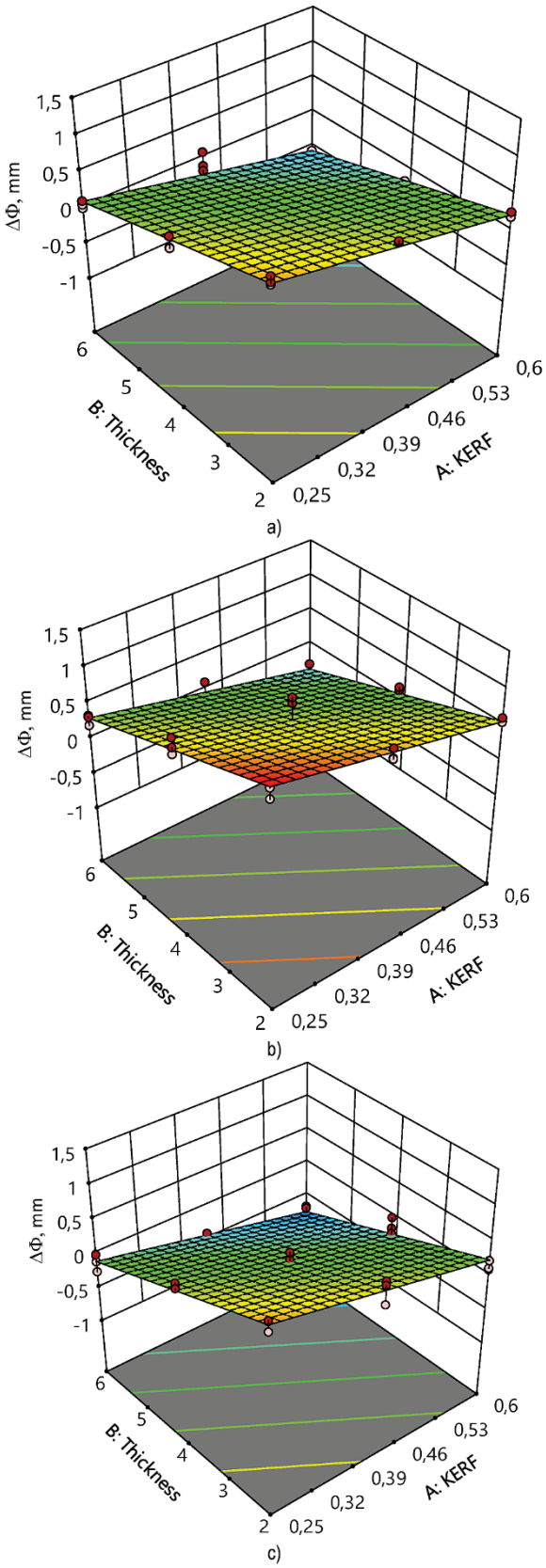

Figure 6 Response surface for diameter: a) Structural steel, b) Aluminum, c) Stainless steel

Tab. 3 shows the values of the variable factor that give optimal or near optimal solution. It can be observed that for certain thicknesses and materials, multiple solutions are considered as optimal, meaning that several different values of the variable factor can give slightly larger deviations in one dimension and slightly smaller deviations in another dimension.

Table 3 Optimal solutions for minimal overall dimensional deviation

Material	Thickness (mm)	Kerf (mm)	Δx (mm)	Δy (mm)	$\Delta \Phi$ (mm)
Con. steel	2	0.382	0.251	0.075	0.660
Con. steel	2	0.379	0.247	0.071	0.665
Con. steel	2	0.386	0.259	0.083	0.652
Con. steel	4	0.420	0.000	0.019	0.180
Con. steel	6	0.479	0.184	0.000	-0.340
Aluminum	2	0.494	0.470	0.153	0.767
Aluminum	4	0.454	0.000	0.220	0.377
Aluminum	6	0.452	0.000	0.357	-0.088
Stainless steel	2	0.372	0.294	0.146	0.689
Stainless steel	2	0.369	0.290	0.142	0.693
Stainless steel	2	0.374	0.298	0.150	0.685
Stainless steel	4	0.531	0.000	0.101	-0.133
Stainless steel	6	0.600	-0.067	-0.112	-0.777

It is possible to determine the optimal size of the variable factor by considering specific constraints and requirements. These constraints and requirements may have different priorities depending on the situation. For instance, the dimensional precision of the bore can be prioritized over the linear dimensions during the optimization process.

As previously stated, higher machine accuracy reduces the time required for final machining of cut specimens and welding positions during assembly. In addition to time, increasing machine accuracy also saves additional material during final machining and welding. Finally, because of the optimisation of the available machines time and material savings contribute to reducing of costs and increasing production efficiency without a significant money investment.

4 CONCLUSION

After completing the statistical analysis of results, multiple significant features were discovered in the specific CNC plasma machine. Initially, it was observed that the y-axis of the machine had significantly lower average deviations, which were related to the machine's design. The console that enables movement along the y-axis contains two parallel guides, both made from one piece, while movement along the x-axis is enabled by one pair of guides, each composed of multiple pieces. Deviations in bore dimensions were significantly larger than deviations in external dimensions of cut specimens, which is an obvious result of the combined action of both axes during bore cutting and the accumulation of their individual inaccuracies. Structural and stainless steel showed the best accuracy for a thickness of 4 mm, while aluminum had the best results for a thickness of 6 mm. Optimal cutting depths were determined for the thicknesses being cut, and equations were derived to predict deviations if cutting thicknesses outside the experimental range is required. All observed features can help the operator in planning the machining process, i.e., entering the cutting

depth into the computer unit and positioning the cut specimens according to dimensional accuracy requirements.

A logical continuation of this research would be to cut materials of thicknesses outside the experimental range and compare the mathematically calculated deviations with the actual ones. Additional opportunities for timesavings and increased accuracy of the machine were identified during the experiment, such as:

- Machine levelling
- Replacing the mesh structure of the table on which the workpieces are placed to reduce the possible waviness
- Updating the software package on the control computer unit to include a cutting depth library, which would eliminate the need for manual input before running the program.

5 REFERENCES

[1] Patel, J. A., Patel, K. H., Prajapati, C. B., Patel, M. D., & Prajapati, R. B. (2014). A Review paper on Experimental Investigation of Plasma Arc Cutting by Full Factorial Design. *International Journal of Software & Hardware Research in Engineering, 2*(9), 22-25.

[2] Gani, A., Ion, W., & Yang, E. (2021). Experimental Investigation of Plasma Cutting Two Separate Thin Steel Sheets Simultaneously and Parameters Optimisation Using Taguchi Approach. *Journal of Manufacturing Processes, 64*, 1013-1023. https://doi.org/10.1016/j.jmapro.2021.01.055

[3] Lazarevic, A. & Lazarevic, D. (2022). Effects of plasma arc cutting process parameters on the cutting speed optimization based on the required cut quality. *CIRP Journal of Manufacturing Science and Technology, 38*, 836-843. https://doi.org/10.1016/j.cirpj.2022.07.003

[4] Maity, K. P. & Bagal, D. K. (2015). Effect of process parameters on cut quality of stainless steel of plasma arc cutting using hybrid approach. *International Journal of Advanced Manufacturing Technology, 78*, 161-175. https://doi.org/10.1007/s00170-014-6552-6

[5] Kechagias, J. D., Petousis, M. A., Vidakis, N., & Mastorakis, N. E. (2017). Plasma Arc Cutting Dimensional Accuracy Optimization employing the Parameter Design approach. *ITM Web of Conferences, 9*, Article No. 03004. https://doi.org/10.1051/itmconf/20170903004

[6] Sharma, D. N. & Kumar, J. R. (2020). Optimization of dross formation rate in plasma arc cutting process by response surface method. *Materials Today: Proceedings, 32*(3), 354-357. https://doi.org/10.1016/j.matpr.2020.01.605

[7] Nemchinsky, V. A. & Severance, W. S. (2009). Plasma arc cutting: Speed and cutting quality. *Journal of Physics D: Applied Physics, 42*, 195204. https://doi.org/10.1088/0022-3727/42/19/195204

[8] Peko, I., Nedić, B., Đorđević, A., & Veža, I. (2018). Modelling of Kerf Width in Plasma Jet Metal Cutting Process using ANN Approach. *Tehnički vjesnik, 25*(2), 401-406. https://doi.org/10.17559/TV-20161024093323

[9] Kumar, P., Kumar, P., & Singh, R. K. (2018). Optimization of plasma cutting parameters for austenitic stainless steel using response surface methodology. *Journal of Manufacturing Processes, 36*, 292-304. https://doi.org/10.1016/j.jmapro.2018.09.016

[10] Feldshtein, E., Patalas-Maliszewska, J., Kłos, S., Kałasznikow, A., & Andrzejewski, K. (2018). The use of Plackett-Burman plans and the analysis of expert opinions, in order to assess the significance of controllable parameters of the plasma cutting process. *Eksploatacja i Niezawodność – Maintenance and Reliability, 20*(3), 443-449. https://doi.org/10.17531/ein.2018.3.13

Authors' contacts:

Hrvoje Cajner, Associate Professor
(Corresponding author)
University of Zagreb,
Faculty of Mechanical Engineering and Naval Architecture,
Ivana Lucica 5, Zagreb, Croatia
hrvoje.cajner@fsb.hr

Vid Križanić, mag. ing, mech.
University of Zagreb,
Faculty of Mechanical Engineering and Naval Architecture,
Ivana Lucica 5, Zagreb, Croatia

Tihomir Opetuk, Assistant Professor
University of Zagreb,
Faculty of Mechanical Engineering and Naval Architecture,
Ivana Lucica 5, Zagreb, Croatia
tihomir.opetuk@fsb.hr

Maja Trstenjak, Postdoctoral Researcher
University of Zagreb,
Faculty of Mechanical Engineering and Naval Architecture,
Ivana Lucica 5, Zagreb, Croatia
maja.trstenjak@fsb.hr